

**UCC Library and UCC researchers have made this item openly available.
 Please [let us know](#) how this has helped you. Thanks!**

| | |
|------------------------------------|---|
| Title | Impact of second-order piezoelectricity on electronic and optical properties of c-plane In _x Ga _{12x} N quantum dots: consequences for long wavelength emitters |
| Author(s) | Patra, Saroj K.; Schulz, Stefan |
| Publication date | 2017-09-05 |
| Original citation | Patra, S. K. and Schulz, S. (2017) 'Impact of second-order piezoelectricity on electronic and optical properties of c-plane In _x Ga _{12x} N quantum dots: consequences for long wavelength emitters', Applied Physics Letters, 111(10), 103103 (5pp). doi:10.1063/1.4991720 |
| Type of publication | Article (peer-reviewed) |
| Link to publisher's version | http://dx.doi.org/10.1063/1.4991720 Access to the full text of the published version may require a subscription. |
| Rights | © 2017, the Authors. Published by AIP Publishing. This article may be downloaded for personal use only. Any other use requires prior permission of the authors and AIP Publishing. The following article appeared in Patra, S. K. and Schulz, S., Applied Physics Letters, 111(10), 103103 (5pp), and may be found at http://dx.doi.org/10.1063/1.4991720 |
| Embargo information | Access to this article is restricted until 12 months after publication by request of the publisher. |
| Embargo lift date | 2018-09-05 |
| Item downloaded from | http://hdl.handle.net/10468/5748 |

Downloaded on 2021-09-24T12:49:33Z

Impact of second-order piezoelectricity on electronic and optical properties of c-plane $\text{In}_x\text{Ga}_{1-x}\text{N}$ quantum dots: Consequences for long wavelength emitters

Saroj Kanta Patra, and Stefan Schulz

Citation: *Appl. Phys. Lett.* **111**, 103103 (2017);

View online: <https://doi.org/10.1063/1.4991720>

View Table of Contents: <http://aip.scitation.org/toc/apl/111/10>

Published by the [American Institute of Physics](#)

Articles you may be interested in

[Molecular beam epitaxial growth and characterization of AlN nanowall deep UV light emitting diodes](#)

Applied Physics Letters **111**, 101103 (2017); 10.1063/1.4989551

[Evolution of threading dislocations in GaN epitaxial laterally overgrown on GaN templates using self-organized graphene as a nano-mask](#)

Applied Physics Letters **111**, 102105 (2017); 10.1063/1.4998924

[Impact of carrier localization on recombination in InGaN quantum wells and the efficiency of nitride light-emitting diodes: Insights from theory and numerical simulations](#)

Applied Physics Letters **111**, 113501 (2017); 10.1063/1.5002104

[Structural and optical characterization of AlGaIn multiple quantum wells grown on semipolar \(20-21\) bulk AlN substrate](#)

Applied Physics Letters **111**, 111101 (2017); 10.1063/1.4985156

[High-performance ultraviolet photodetectors based on lattice-matched InAlN/AlGaIn heterostructure field-effect transistors gated by transparent ITO films](#)

Applied Physics Letters **111**, 102106 (2017); 10.1063/1.4986311

[Deep-UV emission at 219 nm from ultrathin MBE GaN/AlN quantum heterostructures](#)

Applied Physics Letters **111**, 091104 (2017); 10.1063/1.5000844

Scilight

Sharp, quick summaries **illuminating**
the latest physics research

Sign up for **FREE!**



Impact of second-order piezoelectricity on electronic and optical properties of c -plane $\text{In}_x\text{Ga}_{1-x}\text{N}$ quantum dots: Consequences for long wavelength emitters

Saroj Kanta Patra^{1,2,a)} and Stefan Schulz²

¹Department of Electrical Engineering, University College Cork, Cork, Ireland

²Tyndall National Institute, Lee Maltings, Dyke Parade, Cork, Ireland

(Received 22 June 2017; accepted 22 August 2017; published online 5 September 2017)

In this work, we present a detailed analysis of the second-order piezoelectric effect in c -plane $\text{In}_x\text{Ga}_{1-x}\text{N}/\text{GaN}$ quantum dots and its consequences for electronic and optical properties of these systems. Special attention is paid to the impact of increasing In content x on the results. We find that in general the second-order piezoelectric effect leads to an increase in the electrostatic built-in field. Furthermore, our results show that for an In content $\geq 30\%$, this increase in the built-in field has a significant effect on the emission wavelength and the radiative lifetimes. For instance, at 40% In, the radiative lifetime is more than doubled when taking second-order piezoelectricity into account. Overall, our calculations reveal that when designing and describing the electronic and optical properties of c -plane $\text{In}_x\text{Ga}_{1-x}\text{N}/\text{GaN}$ quantum dot based light emitters with high In contents, second-order piezoelectric effects cannot be neglected. *Published by AIP Publishing.*
<http://dx.doi.org/10.1063/1.4991720>

Heterostructures based on $\text{In}_x\text{Ga}_{1-x}\text{N}$ alloys are of great technological interest thanks to their bandgap energy E_g tunability with changing In content x .^{1–3} By changing x , in principle, wavelengths between the ultraviolet ($E_g^{\text{GaN}} \approx 3.5$ eV) and the near infrared regime ($E_g^{\text{InN}} \approx 0.67$ eV) are achievable. Thus, this ideally broad range spans the entire visible spectrum, rendering the material highly suitable for use in optoelectronic devices such as light-emitting diodes, laser diodes, and solar cells.^{1–3} Utilizing $\text{In}_x\text{Ga}_{1-x}\text{N}/\text{GaN}$ based quantum well (QW) structures, high efficiency devices operating in the violet and blue spectral regions have been realized over the last few years.^{4,5} However, keeping the efficiency high and extending the emission wavelength into the green, yellow, or infrared wavelength range by increasing the In content x , is still challenging.^{6,7} Several factors contribute to this so-called “green gap” problem,⁸ ranging from sample quality, due to large strains in QW systems, up to strong strain-induced electrostatic piezoelectric fields. The piezoelectric effect leads, for instance, to a spatial separation of electron and hole wave functions and in turn to increased radiative lifetimes, also known as the quantum confined Stark effect (QCSE).⁹ However, theoretical studies have shown that the built-in field is strongly reduced in an $\text{In}_x\text{Ga}_{1-x}\text{N}/\text{GaN}$ quantum dot (QD) when compared to a QW of the same height and In content.¹⁰ This originates from strain relaxation mechanism and surface area effects, stemming from the three dimensional QD confinement, and results in a reduction of the QCSE in QDs. Therefore, for an $\text{In}_x\text{Ga}_{1-x}\text{N}/\text{GaN}$ QD, when compared to an $\text{In}_x\text{Ga}_{1-x}\text{N}/\text{GaN}$ QW of the same height, the In content x in the dot can be increased considerably for a comparable field in both systems. This suggests that $\text{In}_x\text{Ga}_{1-x}\text{N}/\text{GaN}$ QDs are promising candidates to achieve efficient radiative recombination at longer wavelengths. Recently, making use of this concept,

$\text{In}_x\text{Ga}_{1-x}\text{N}/\text{GaN}$ QD based light emitters operating in the green to yellow spectral range have been realized.^{11,12} Moreover, Frost and co-workers^{13,14} have demonstrated high performance red emitting (>630 nm) lasers using $\text{In}_x\text{Ga}_{1-x}\text{N}/\text{GaN}$ QDs. To achieve this emission wavelength, In contents as high as 40% have been reported.¹³ Only a few theoretical studies have addressed the electronic and optical properties of these high In content, long wavelength emitters.^{14,15} Additionally, piezoelectric fields in thin InN layers, embedded in GaN, have been used to achieve topological insulator states.¹⁶ However, all previous theoretical studies on these different aspects of InGaN/GaN based systems included linear piezoelectric polarization contributions only. Recently, non-linear piezoelectricity effects have been discussed and reported for wurtzite III-N QW systems.^{17–19} These studies showed for instance better agreement between theoretical and experimental built-in field values when second-order piezoelectric effects are considered in the calculations. Furthermore, in other material systems, such as zincblende InAs/GaAs QDs, second-order piezoelectric effects have been highlighted to affect their electronic and optical properties significantly.^{20–22} But, no detailed study exists on the importance of second-order piezoelectricity on electronic and optical properties of c -plane $\text{In}_x\text{Ga}_{1-x}\text{N}$ dots with varying In contents. Given the recent drive for $\text{In}_x\text{Ga}_{1-x}\text{N}$ QD based light emitters with high In contents ($x \approx 0.4$), the question of how important second-order piezoelectric effects are for describing and designing these emitters for future optoelectronic devices is of central importance.

Here, we address this question by calculating electronic and optical properties of c -plane $\text{In}_x\text{Ga}_{1-x}\text{N}/\text{GaN}$ QDs with In contents ranging from 10% to 50% using a continuum based model, which includes the full second-order piezoelectric polarization vector. We find that the second-order piezoelectric effect leads to an increase in the electrostatic built-in field when compared to the situation where only standard first-order (FO) contributions are accounted for. This increase in the

^{a)}Electronic mail: sarojkanta.patra@tyndall.ie

built-in field, at least for the structures studied here, is of secondary importance for emission wavelength and radiative lifetime of c -plane dots with In contents in the range of 10%–20%. However, for In contents of order 40%, our calculations show that second-order piezoelectricity has a significant effect on these quantities. For instance, at $x = 0.4$, we observe that for the chosen QD geometry, the radiative lifetime is more than doubled when comparing a calculation that includes second-order piezoelectric effects to one neglecting this contribution. Consequently, second-order piezoelectricity has to be taken into account when designing nanostructures operating in the long wavelength, high In content regime.

The total strain induced piezoelectric polarization ($\mathbf{P}_{\text{pz}}^{\text{Tot}}$) in a semiconductor material with a lack of inversion symmetry can be written, up to second-order, as²⁰

$$P_{\text{pz},\mu}^{\text{Tot}} = P_{\text{pz},\mu}^{\text{FO}} + P_{\text{pz},\mu}^{\text{SO}} = \sum_{j=1}^6 e_{\mu j} \epsilon_j + \frac{1}{2} \sum_{j,k=1}^6 B_{\mu jk} \epsilon_j \epsilon_k. \quad (1)$$

$$\mathbf{P}_{\text{pz}}^{\text{Tot}} = \begin{pmatrix} 2e_{15}\epsilon_{xz} \\ 2e_{15}\epsilon_{yz} \\ e_{31}(\epsilon_{xx} + \epsilon_{yy}) + e_{33}\epsilon_{zz} \end{pmatrix} + \begin{pmatrix} 2B_{115}(\epsilon_{xx}\epsilon_{xz} + \epsilon_{xy}\epsilon_{yz}) + 2B_{135}\epsilon_{zz}\epsilon_{xz} - 2B_{125}(\epsilon_{xy}\epsilon_{yz} - \epsilon_{yy}\epsilon_{xz}) \\ 2B_{115}(\epsilon_{yy}\epsilon_{yz} + \epsilon_{xy}\epsilon_{xz}) + 2B_{135}\epsilon_{zz}\epsilon_{yz} + 2B_{125}(\epsilon_{xx}\epsilon_{yz} - \epsilon_{xy}\epsilon_{xz}) \\ \frac{B_{311}}{2}(\epsilon_{xx}^2 + \epsilon_{yy}^2 + 2\epsilon_{xy}^2) + B_{312}(\epsilon_{xx}\epsilon_{yy} - \epsilon_{xy}^2) + B_{313}(\epsilon_{xx}\epsilon_{zz} + \epsilon_{yy}\epsilon_{zz}) + 2B_{344}(\epsilon_{yz}^2 + \epsilon_{xz}^2) + \frac{B_{333}}{2}\epsilon_{zz}^2 \end{pmatrix}. \quad (2)$$

It should be noted that this expression is far more complicated when compared to piezoelectric effects in zincblende structures. In the zincblende case, one is left with only one first-order and three independent second-order piezoelectric coefficients.^{20,24}

To analyze the impact of second-order piezoelectricity on the electronic and optical properties of c -plane $\text{In}_x\text{Ga}_{1-x}\text{N}/\text{GaN}$ QDs with varying In content x , we have performed continuum-based calculations by means of $\mathbf{k} \cdot \mathbf{p}$ theory. All calculations have been carried out in the highly flexible plane wave based software library S/PHI/nX,²⁵ allowing us to define customized piezoelectric polarization vector fields such as Eq. (2). In doing so, we are able to perform calculations in the presence and absence of second-order piezoelectricity. Additionally, spontaneous polarization (SP) effects are included in the calculations, with values for GaN and InN taken from Ref. 26 and the bowing parameter from Ref. 27. First-order piezoelectric coefficients from Ref. 26 and second-order coefficients from Ref. 18 have been used. For the electronic structure calculations, we have applied a six-band Hamiltonian to describe hole states and a single-band effective mass approximation for electron states. This model accounts for valence band mixing effects and the differences in the effective masses along different directions. Since we are mainly interested in, e.g., wavelength shifts due to second-order piezoelectricity, the applied electronic structure approach is sufficient for our purposes. Further refinements can be achieved by applying an eight-band model.¹⁶ Using the $\mathbf{k} \cdot \mathbf{p}$ wave functions, the radiative lifetime τ of the

Here, $P_{\text{pz},\mu}^{\text{FO}} = \sum_{j=1}^6 e_{\mu j} \epsilon_j$ is the first order contribution and $P_{\text{pz},\mu}^{\text{SO}} = \frac{1}{2} \sum_{j,k=1}^6 B_{\mu jk} \epsilon_j \epsilon_k$ is the second-order part. The first-order piezoelectric coefficients are denoted by $e_{\mu j}$ and $B_{\mu jk}$ are second-order ones. The strain tensor components (in Voigt notation) are given by ϵ_j . From Eq. (1), one can infer already that second-order piezoelectricity should become important for systems under large strains, in our case high In contents, given that it is related to products of strain tensor components.

For wurtzite semiconductors, the well known first-order contribution $\mathbf{P}_{\text{pz}}^{\text{FO}}$ has only three independent piezoelectric coefficients, namely, e_{33} , e_{15} , and e_{31} .²³ For the second-order coefficients $B_{\mu jk}$, Grimmer²⁴ showed that out of 36 $B_{\mu jk}$ coefficients, 17 are nonzero of which 8 are independent. Taking all this into account and using Cartesian notation for the strain tensor, in a wurtzite c -plane system the total (first- plus second-order) piezoelectric polarization vector field $\mathbf{P}_{\text{pz}}^{\text{Tot}}$ is given by

electron and hole ground state transition has been calculated,^{28,29} employing a light polarization vector \mathbf{e} perpendicular to the sample surface. More details on theoretical framework and parameter sets applied are given in Refs. 25, 28, 30, and 31.

Following previous studies on $\text{In}_x\text{Ga}_{1-x}\text{N}$ QDs, we have assumed a lens-shaped dot geometry.^{10,32} Based on earlier atomic force microscopy results, a QD base diameter of $d = 14$ nm and a dot height of $h = 3$ nm have been chosen.^{33,34} Here, our main focus is on how electronic and optical properties of c -plane $\text{In}_x\text{Ga}_{1-x}\text{N}$ QDs change with increasing In content x when second-order piezoelectric effects are considered. Thus, we vary the In content x of the dot between 10% and 50% in 10% steps.

In a first step, we analyze how the built-in potential in a c -plane $\text{In}_x\text{Ga}_{1-x}\text{N}/\text{GaN}$ QD is changed when including second-order piezoelectric effects. Contour plots of the built-in potential of a c -plane $\text{In}_{0.5}\text{Ga}_{0.5}\text{N}/\text{GaN}$ dot, for a slice through the QD center, are shown in Fig. 1. The slice is taken in the x - z -plane, where the z -axis is parallel to the wurtzite c -axis. The impact of changes in the In content x will be investigated below when we discuss electronic and optical properties of the structures under consideration. In Fig. 1(a), the built-in potential arising from the standard first-order piezoelectric contribution and the spontaneous polarization is shown. The well known potential drop along the c -axis, leading to a spatial separation of electron and hole wave functions, is clearly visible. Figure 1(b) depicts the second-order piezoelectric contribution only. Here, several features are of

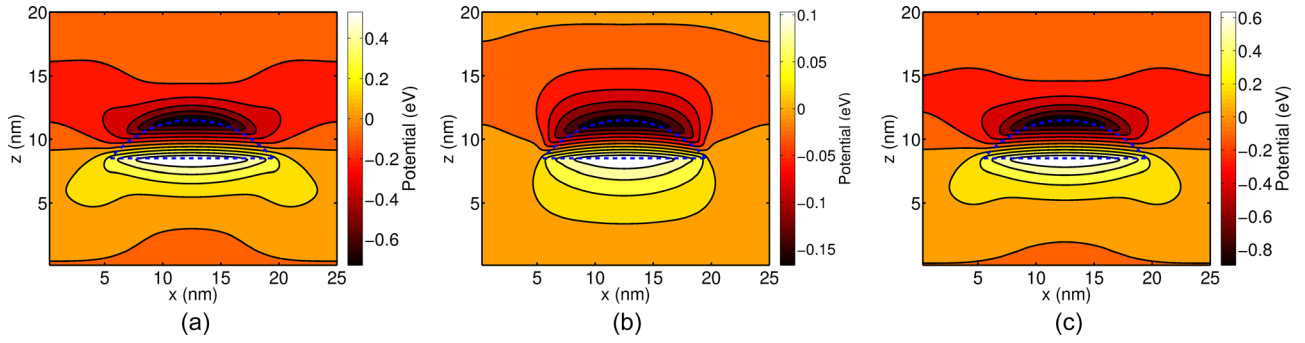


FIG. 1. (a) Contour plot of the built-in potential arising from spontaneous and first-order piezoelectric polarization in a lens-shaped $\text{In}_{0.5}\text{Ga}_{0.5}\text{N}/\text{GaN}$ c -plane dot with a base diameter $d = 14$ nm and a height $h = 3$ nm. The contour plot is shown for a slice through the center of the dot in the x - z plane. (b) The same as in (a) but here second-order piezoelectric effects only are considered. (c) The same as in (a) but the total (spontaneous + first-order + second-order) built-in potential is shown.

interest. First, the magnitude of the second-order contribution, even at $x = 0.5$, is a factor of order 4 smaller compared to the situation where only first-order piezoelectricity and spontaneous polarization are taken into account [cf. Fig. 1(a)]. Nevertheless, the second-order contribution has still a sizeable magnitude. Second, the symmetry of the second-order contribution and the potential profile are similar to the first-order contribution [cf. Fig. 1(a)]. Thus, when taking second-order piezoelectric effects into account, the potential drop across the QD will be larger, leading to an even stronger electrostatic built-in field and thus to an even stronger spatial separation of electron and hole wave functions. We will come back to this effect below. The fact that the second-order built-in potential contribution is of the same symmetry as the first-order term is for instance different to zincblende InAs/GaAs QDs.²⁰ Additionally, it should be noted that the magnitude of the second-order piezoelectric contribution also depends on the QD shape and size, as highlighted by Schliwa *et al.*²² for $\text{InGaAs}/\text{GaAs}$ QD systems. To gain initial insights into this question for InGaN QDs, we have performed additional calculations for a slightly larger dot ($d = 18$ nm, $h = 3$ nm) with 30% In. This study reveals only a slight increase in the potential drop across the nanostructure when compared to an $\text{In}_{0.3}\text{Ga}_{0.7}\text{N}$ dot with $d = 14$ nm and $h = 3$ nm. For different QD geometries and/or higher dots, this situation might change. However, a detailed analysis of the impact of QD shape and size is beyond the scope of the present study. Here, we are interested in establishing trends with increasing In content. Figure 1(c) shows the total (spontaneous + first-order + second-order) built-in potential for the considered lens-shaped c -plane $\text{In}_{0.5}\text{Ga}_{0.5}\text{N}$ QD. As expected from the discussion above, when including second-order piezoelectric effects, the total potential drop is clearly increased compared to the situation where only first-order piezoelectricity and spontaneous polarization are included [cf. Fig. 1(a)]. The question is now how strongly are electronic and optical properties affected when taking second-order piezoelectric effects into account? In the following, we will look at the impact of second-order piezoelectricity on the emission wavelength λ and the radiative lifetime τ as a function of the dot In content x . But before turning to these questions, we start with looking at the electron and hole ground state charge densities of the $\text{In}_{0.5}\text{Ga}_{0.5}\text{N}/\text{GaN}$ QD. Figure 2 shows the isosurfaces of the electron (red) and hole (green)

ground state charge densities. In Fig. 2(a), results in the absence of the second-order piezoelectric effect are shown; (b) depicts data originating from a calculation accounting for the full built-in potential, thus including second-order piezoelectricity. From Fig. 2, we can conclude that the increase in the built-in potential due to second-order piezoelectricity leads to a stronger spatial separation of the carriers along the c -axis. Thus, the wave function overlap is reduced and consequently the radiative lifetime will increase. Also, due to the increased built-in potential, an increased red shift of the emission wavelength due to second-order piezoelectricity is expected.

Figure 3 shows the emission wavelength λ of the here considered c -plane $\text{In}_x\text{Ga}_{1-x}\text{N}/\text{GaN}$ QD for In contents varying between 10% and 50%. The black squares ($\lambda^{\text{FO+SP}}$) denote the results in the absence of second-order contributions [only first-order (FO) piezoelectricity and spontaneous (SP) polarization], while the red circles (λ^{Tot}) show the data when including also second-order piezoelectric effects. Again, it should be noted that for emitters operating in the

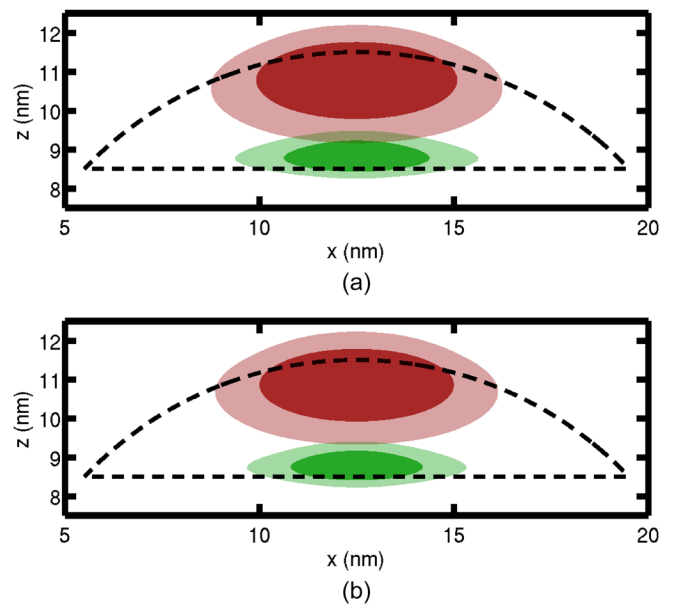


FIG. 2. Isosurface plots of the electron (red) and hole (green) ground state charge densities at 5% (light surface) and 25% (dark surface). The QD geometry is indicated by the dashed line. (a) Built-in potential due to spontaneous and first-order piezoelectric polarization only. (b) Full built-in potential.

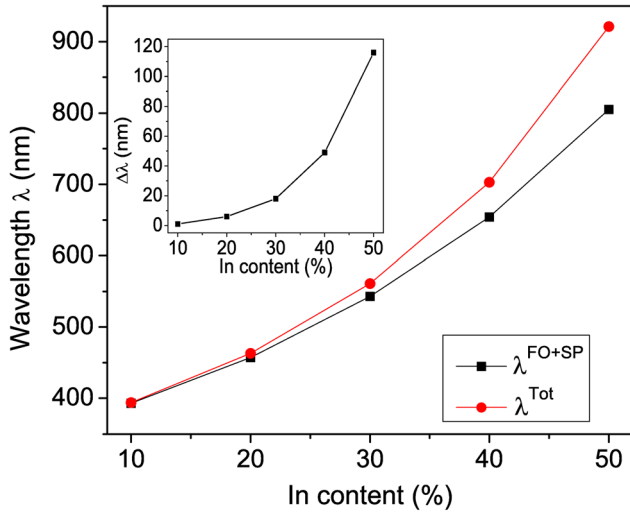


FIG. 3. Emission wavelength λ as a function of In content. Results in the absence of second-order piezoelectricity, taking only spontaneous (SP) and first-order (FO) piezoelectric polarization into account, are given by the black squares ($\lambda^{\text{FO+SP}}$). The red circles denote data when including second-order piezoelectricity (λ^{Tot}). The inset shows $\Delta\lambda = \lambda^{\text{Tot}} - \lambda^{\text{FO+SP}}$.

red wavelength regime, In contents of 40% have been reported in the literature,¹³ so that the here studied In content range is relevant to recent experimental studies. From Fig. 3, one can infer that for lower In contents (up to 20%), the second-order piezoelectric contribution has little effect on λ . In fact in this case the difference in the emission wavelength $\Delta\lambda = \lambda^{\text{Tot}} - \lambda^{\text{FO+SP}}$, obtained from a calculation with spontaneous and first-order piezoelectric polarization only, $\lambda^{\text{FO+SP}}$, and a calculation including second-order piezoelectric effects, λ^{Tot} , is less than 10 nm. To show this effect more clearly, the inset in Fig. 3 depicts $\Delta\lambda$ as a function of the In content x . Between 30% and 40% In, second-order effects lead to a noticeable difference, resulting in $\Delta\lambda$ values of approximately 20 nm to 50 nm, respectively. At 50% In, we observe a wavelength shift of $\Delta\lambda = 120$ nm. Overall, the wavelength shift is almost equally distributed between electron and hole ground state energy shifts. We attribute this to the combined effect of differences in electron and hole effective masses and the asymmetry in the magnitude of the built-in potential between the upper and lower QD interface. Moreover, the change in the confinement potential due to second-order piezoelectricity might also affect the Coulomb interaction between the carriers and can lead to further contributions to the wavelength shift discussed here in the single-particle picture. Overall, our calculations reveal two things. First, when targeting QD-based emitters operating in the red spectral regime (≈ 650 nm), second-order piezoelectric effects can play a significant role. Furthermore, the second-order piezoelectric contribution shifts the emission to longer wavelength. Thus, when designing emitters operating in this long wavelength regime, the required In content predicted from a model including second-order effects would be lower as expected from a “standard model”, which accounts for first-order piezoelectric effects and spontaneous polarization only.

Even though our analysis indicates that lower In contents are sufficient to reach emission at longer wavelength, the increase in the built-in potential responsible for this

effect will have a detrimental effect on the wave function overlap and consequently on the radiative lifetime τ . To study the impact of second-order piezoelectricity on the radiative lifetime τ , Fig. 4 depicts τ in the absence ($\tau^{\text{FO+SP}}$, black squares) and in the presence (τ^{Tot} , red circles) of second-order piezoelectric contributions. Similar to the wavelength shift discussed above, in the In content range of 10% to 20%, the influence of second-order piezoelectricity is of secondary importance ($\Delta\tau \leq 2$ ns). The inset of Fig. 4 depicts the difference in the radiative lifetime $\Delta\tau = \tau^{\text{Tot}} - \tau^{\text{FO+SP}}$, obtained from calculations including (τ^{Tot}) and neglecting ($\tau^{\text{FO+SP}}$) second-order piezoelectric contributions. The calculated radiative lifetimes in the 10% to 20% In regime are in the range of 3 ns to 10 ns, which is in good agreement with reported experimental data on these systems.^{35,36} However, for higher In contents, we clearly observe a significant contribution from second-order piezoelectricity. At 30%, the τ value is a factor of order 1.5 larger ($\tau^{\text{FO+SP}} = 12$ ns; $\tau^{\text{Tot}} = 19$ ns) when including second-order piezoelectric effects in the calculations. At 40% and 50% In, the value of $\Delta\tau$ becomes 23 ns and 62 ns, respectively. But, it should be noted that the here calculated radiative lifetimes for a c -plane $\text{In}_{0.4}\text{Ga}_{0.6}\text{N}$ QD, even without second-order effects, are much larger than the experimental values ($\tau^{\text{exp}} = 3$ ns) reported in the literature for InGaN dots with 40% In.¹³ Further studies, both theoretically and experimentally, are required to shed more light onto the physics of $\text{In}_x\text{Ga}_{1-x}\text{N}$ QDs operating in the long wavelengths regime (green to red).

In summary, we have presented a detailed analysis of the impact of second-order piezoelectricity on the electronic and optical properties of c -plane $\text{In}_x\text{Ga}_{1-x}\text{N}/\text{GaN}$ QDs. Our study revealed that the second-order piezoelectric effect leads to an increase in the built-in field when compared to calculations taking only first-order piezoelectricity and spontaneous polarization into account. However, when looking at emission wavelength shifts or radiative lifetime values, at In

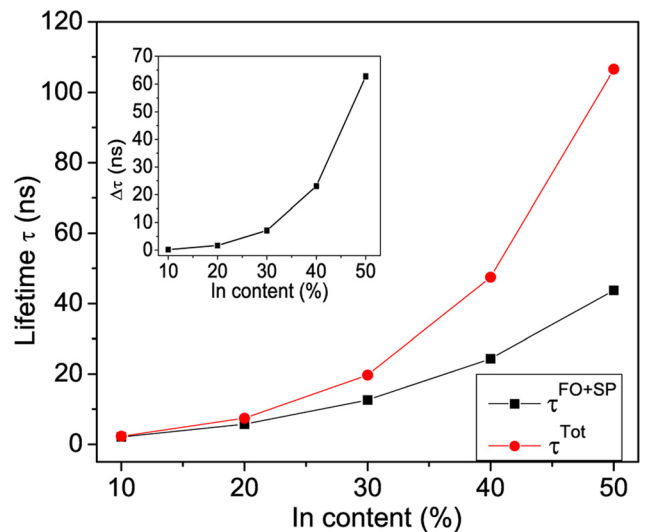


FIG. 4. Radiative lifetime τ as a function of In content. Results in the absence of second-order piezoelectricity, including spontaneous (SP) and first-order (FO) piezoelectric polarization only, are given by the black squares ($\tau^{\text{FO+SP}}$). The red circles denote the data when including second-order piezoelectricity (τ^{Tot}). The inset shows $\Delta\tau = \tau^{\text{Tot}} - \tau^{\text{FO+SP}}$.

contents around 10% to 20%, these quantities are almost unaffected by second-order piezoelectricity. But, when exceeding 30% In, both quantities are affected significantly by second-order contributions. The second-order piezoelectric effect induced built-in field increase leads to the situation that the emission is shifted to longer wavelength in comparison to a calculation based on spontaneous and first-order piezoelectric polarization effects only. This means that when accounting for second-order piezoelectric effects, lower In contents can be considered to reach for instance emission in the red spectral region. On the other hand, the increase in the built-in potential due to second-order piezoelectric contributions results in a strong increase in the radiative lifetime for long wavelength, high In content emitters when compared to results from a “standard” first-order study. Overall, our results reveal that when targeting $\text{In}_x\text{Ga}_{1-x}\text{N}/\text{GaN}$ QD-based emitters operating in the yellow to red spectral regime, second-order piezoelectricity cannot be neglected and should be taken into account for designing and understanding the electronic and optical properties of these systems.

This work was supported by Science Foundation Ireland (Project No. 13/SIRG/2210). The authors would like to thank Brian Corbett, Eoin P. O’Reilly, and Miguel A. Caro for fruitful discussions.

- ¹S. Nakamura, M. Senoh, S. Ichi Nagahama, N. Iwasa, T. Yamada, T. Matsushita, H. Kiyoku, and Y. Sugimoto, *Jpn. J. Appl. Phys., Part 2* **35**, L74 (1996).
- ²E. Matioli, C. Neufeld, M. Iza, S. C. Cruz, A. A. Al-Heji, X. Chen, R. M. Farrell, S. Keller, S. DenBaars, U. Mishra, S. Nakamura, J. Speck, and C. Weisbuch, *Appl. Phys. Lett.* **98**, 021102 (2011).
- ³S. Nakamura and G. Fasol, *The Blue Laser Diode* (Springer, 1997).
- ⁴S. Nakamura, *Rev. Mod. Phys.* **87**, 1139 (2015).
- ⁵H. Shen, W. Cao, N. T. Shewmon, C. Yang, L. S. Li, and J. Xue, *Nano Lett.* **15**, 1211 (2015).
- ⁶Y. Jiang, Y. Li, Y. Li, Z. Deng, T. Lu, Z. Ma, P. Zuo, L. Dai, L. Wang, H. Jia, W. Wang, J. Zhou, W. Liu, and H. Chen, *Sci. Rep.* **5**, 10883 (2015).
- ⁷C. Du, Z. Ma, J. Zhou, T. Lu, Y. Jiang, P. Zuo, H. Jia, and H. Chen, *Appl. Phys. Lett.* **105**, 071108 (2014).
- ⁸C. Humphreys, J. Griffiths, F. Tang, F. Oehler, S. Findlay, C. Zheng, J. Etheridge, T. Martin, P. Bagot, M. Moody, D. Sutherland, P. Dawson, S. Schulz, S. Zhang, W. Fu, T. Zhu, M. Kappers, and R. Oliver, *Ultramicroscopy* **176**, 93 (2017).
- ⁹S. Pu Wan, J. Bai Xia, and K. Chang, *J. Appl. Phys.* **90**, 6210 (2001).

- ¹⁰S. Schulz and E. P. O’Reilly, *Phys. Rev. B* **82**, 033411 (2010).
- ¹¹G. Weng, Y. Mei, J. Liu, W. Hofmann, L. Ying, J. Zhang, Y. Bu, Z. Li, H. Yang, and B. Zhang, *Opt. Express* **24**, 15546 (2016).
- ¹²Y. Mei, G.-E. Weng, B.-P. Zhang, J.-P. Liu, W. Hofmann, L.-Y. Ying, J.-Y. Zhang, Z.-C. Li, H. Yang, and H.-C. Kuo, *Light: Sci. Appl.* **6**, e16199 (2017).
- ¹³T. Frost, A. Hazari, A. Aiello, M. Z. Baten, L. Yan, J. Mirecki-Millunchick, and P. Bhattacharya, *Jpn. J. Appl. Phys., Part 1* **55**, 032101 (2016).
- ¹⁴G.-L. Su, T. Frost, P. Bhattacharya, and J. M. Dallesasse, *Opt. Express* **23**, 12850 (2015).
- ¹⁵M. Khoshnegar, M. Sodagar, A. Eftekharian, and S. Khorasani, *IEEE J. Quantum Electron.* **46**, 228 (2010).
- ¹⁶M. S. Miao, Q. Yan, C. G. Van de Walle, W. K. Lou, L. L. Li, and K. Chang, *Phys. Rev. Lett.* **109**, 186803 (2012).
- ¹⁷J. Pal, G. Tse, V. Haxha, M. A. Migliorato, and S. Tomić, *Phys. Rev. B* **84**, 085211 (2011).
- ¹⁸P.-Y. Prodhomme, A. Beya-Wakata, and G. Bester, *Phys. Rev. B* **88**, 121304 (2013).
- ¹⁹M. A. Migliorato, J. Pal, R. Garg, G. Tse, H. Y. Al-Zahrani, U. Monteverde, S. Tomić, C.-K. Li, Y.-R. Wu, B. G. Crutchley, I. P. Marko, and S. J. Sweeney, *AIP Conf. Proc.* **1590**, 32 (2014).
- ²⁰G. Bester, A. Zunger, X. Wu, and D. Vanderbilt, *Phys. Rev. B* **74**, 081305 (2006).
- ²¹G. Bester, X. Wu, D. Vanderbilt, and A. Zunger, *Phys. Rev. Lett.* **96**, 187602 (2006).
- ²²A. Schliwa, M. Winkelkemper, and D. Bimberg, *Phys. Rev. B* **76**, 205324 (2007).
- ²³A. D. Andreev and E. P. O’Reilly, *Phys. Rev. B* **62**, 15851 (2000).
- ²⁴H. Grimmer, *Acta Crystallogr., Sect. A* **63**, 441 (2007).
- ²⁵O. Marquardt, S. Boeck, C. Freysoldt, T. Hickel, S. Schulz, J. Neugebauer, and E. P. O’Reilly, *Comput. Mater. Sci.* **95**, 280 (2014).
- ²⁶M. A. Caro, S. Schulz, and E. P. O’Reilly, *Phys. Rev. B* **88**, 214103 (2013).
- ²⁷I. Vurgaftman and J. R. Meyer, *J. Appl. Phys.* **94**, 3675 (2003).
- ²⁸S. K. Patra, T. Wang, T. J. Puchtler, T. Zhu, R. A. Oliver, R. A. Taylor, and S. Schulz, *Phys. Status Solidi B* **254**, 1600675 (2017).
- ²⁹V. A. Fonoberov and A. A. Balandin, *J. Appl. Phys.* **94**, 1718 (2003).
- ³⁰S. K. Patra and S. Schulz, *J. Phys. D: Appl. Phys.* **50**, 025108 (2017).
- ³¹S. K. Patra, O. Marquardt, and S. Schulz, *Opt. Quantum Electron.* **48**, 151 (2016).
- ³²S. Barthel, K. Schuh, O. Marquardt, T. Hickel, J. Neugebauer, F. Jahnke, and G. Czycholl, *Eur. Phys. J. B* **86**, 449 (2013).
- ³³O. Moriwaki, T. Someya, K. Tachibana, S. Ishida, and Y. Arakawa, *Appl. Phys. Lett.* **76**, 2361 (2000).
- ³⁴M. S n s, K. L. Smith, T. M. Smeeton, S. E. Hooper, and J. Heffernan, *Phys. Rev. B* **75**, 045314 (2007).
- ³⁵J. W. Robinson, J. H. Rice, A. Jarjour, J. D. Smith, R. A. Taylor, R. A. Oliver, G. A. D. Briggs, M. J. Kappers, C. J. Humphreys, and Y. Arakawa, *Appl. Phys. Lett.* **83**, 2674 (2003).
- ³⁶A. F. Jarjour, R. A. Oliver, A. Tahraoui, M. J. Kappers, C. J. Humphreys, and R. A. Taylor, *Phys. Rev. Lett.* **99**, 197403 (2007).